American Mineralogist, Volume 87, pages 1401–1409, 2002

Experimental determination of calcite solubility in H_2O-NaCl solutions at deep crust/upper mantle pressures and temperatures: Implications for metasomatic processes in shear zones

ROBERT C. NEWTON AND CRAIG E. MANNING*

Department of Earth and Space Sciences, University of California at Los Angeles, Los Angeles, California 90095-1567, U.S.A.

ABSTRACT

The solubility of calcite in NaCl-H_2O solutions was measured at 600–900 °C, 10 kbar, at NaCl concentrations ranging from dilute to near halite saturation, and at 6–14 kbar, 700 °C, in 30 mol% NaCl solutions. Solubility was determined from the weight loss of cleavage rhombs of a pure natural calcite after experiments of 1/2 to 6 days in a piston-cylinder apparatus with NaCl-graphite furnaces. $CaCO_3$ molality (m_{CaCO_3}) increases greatly with NaCl mole fraction (X_{NaCl}): at 800 °C and 10 kbar, m_{CaCO_3} increases from ~0.1 in pure H_2O to near 4.0 at halite saturation ($X_{NaCl} \sim 0.6$). There is also a large temperature effect at 10 kbar, with m_{CaCO_3} increasing from 0.25 at 600 °C to 3.0 at 900 °C at $X_{NaCl} = 0.3$. There is only a 20% increase with increasing pressure between 6 and 14 kbar at 700 °C and $X_{NaCl} = 0.3$. Melting to a carbonate-rich liquid was inferred at 900 °C, 10 kbar, from X_{NaCl} of 0 to 0.2. The composition, temperature, and pressure dependence of m_{CaCO_3} are described by:

$$m_{CaCO_3} = [-0.051 + 1.65 \times 10^{-4}\, T + X_{NaCl}^2 \exp(-3.071 + 4.749 \times 10^{-6} T^2)]\ (0.76 + 0.024P)$$

with T in Kelvins and P in kbar. The predicted increase of calcite solubility with salinity and temperature is so great that critical mixing of NaCl-rich hydrous carbonate liquid and $CaCO_3$-rich saline solution is probable at 10 kbar near 1000 °C and $X_{NaCl} \sim 0.4$.

The experimental results suggest a genetic mechanism for the enigmatic carbonated shear zones, such as the Attur Valley of southern India, where crustal rocks have been replaced by up to 20% by calcite and ankerite with mantle-like stable-isotope signatures. The high $CaCO_3$ carrying capacity of concentrated alkali-chloride solutions, together with the drastic decrease in solubility between 1000 and 700 °C, plausibly account for large-scale emplacement of mantle-derived carbonate from concentrated chloride-carbonate solutions (or hydrosaline magmas) formed as immiscible fluids in the late stages of alkalic magmatism. Such solutions may also mobilize sulfate and phosphate minerals, which would have important consequences for redistribution of incompatible and heat-producing elements in the crust.

INTRODUCTION

Calcite-bearing veins are common in low- to middle-grade metamorphic terranes. Textural interpretation of the sequences of vein formation can provide valuable information on deformational history as recorded in crack-opening and crack-sealing events, as in the French Western Alps (Henry et al. 1996) and in the Southern Alps, New Zealand (Craw et al. 1987). The volumes of emplaced carbonate in these occurrences are generally quite small relative to the host rocks. Fluid inclusion studies have shown that the transporting fluids were mildly saline to nearly pure H_2O in different vein-forming events. Stable isotopes indicate that the fluid sources were intraformational in the French Western Alps and that there were through-connected heterogeneous sources in the Franciscan subduction zone of the Catalina Schist of California (Bebout and Barton 1989).

In contrast to low-grade terranes, several medium- and high-grade areas, typically in large-scale shear zones, display pervasive and vein-controlled carbonate metasomatism of country rock. These areas may be termed carbonated megashear zones. Examples include the post-Hercynian South Tien Shan fault zone (Baratov et al. 1984), the Late Proterozoic Attur Valley of Tamil Nadu, India (Wickham et al. 1994), the Late Archean Chitradurga area of Karnataka, India (Chadwick et al. 1989), the Mid-Proterozoic Mary Kathleen Fold Belt of Queensland, Australia (Oliver et al. 1993), and the Mid-Proterozoic Bamble Shear Belt of southern Norway (Dahlgren et al. 1993). Exposed country rocks in some of these metasomatic zones have been replaced by up to 20% by carbonate over tracts of 100 km by 10 km. The host rocks may be either dominantly metasedimentary, as in the South Tien Shan and Mary Kathleen occurrences, or dominantly orthogneisses, as in the Attur Valley and Bamble occurrences. The isotopic composition of C in calcite and ankerite in the Attur Valley and South Tien Shan occurrences point to a remarkably large and uniform, probably subcrustal source of the metasomatizing fluids. Fluid-inclusion analysis of the Queensland occurrence, as well as profound

* E-mail: manning@ess.ucla.edu

0003-004X/02/0010–1401$05.00

Na-Ca metasomatism of associated non-carbonate-bearing lower-grade rocks indicates that highly saline fluids were involved in the metasomatism there (DeJong and Williams 1995). All of the cited carbonate-replacement events occurred at 500–700 °C and several kbar. The Attur Valley and South Tien Shan occurrences are associated with numerous small intrusions of alkali gabbro, syenite, and carbonatite, which, though much smaller in exposed volumes than the carbonate-metasomatized country rocks, enhance the idea of a mantle origin of the metasomatizing fluids.

Experimental determination of the aqueous solubility of calcite immediately poses a problem for the origin of large-scale carbonate metasomatism. Calcite solubility decreases sharply with increasing temperature along the boiling curve of water (Ellis 1959), and the negative temperature dependence persists at supercritical conditions to 2 kbar and temperatures of 600 °C (Fein and Walther 1987). The calcite solubility at these conditions is only $10^{-4.3}$ mol/kg of H_2O. If the temperature trend can be extrapolated for as little as 100–200 °C, it can be inferred that calcite is one of the most insoluble of common minerals at high-grade metamorphic conditions.

Another factor that must be considered is the low H_2O activity that is necessary in deep-crustal metamorphism if aqueous fluids are to be present and compatible with high-grade mineral assemblages. Fein and Walther (1987) explored the effect of lowering H_2O activity by addition of CO_2 at 400–500 °C and 2 kbar. They found an initial enhancement of calcite solubility for CO_2 mole fractions up to 0.05, but then a rapid decrease in solubility between 0.05 and 0.15 mole fraction CO_2 (X_{CO_2}). Fluids compatible with granulite-facies assemblages would have to have $X_{CO_2} \geq 0.6$ (Aranovich and Newton 1999). If calcite solubility is governed primarily by the stability of the bicarbonate ion, HCO_3^-, the calculations of Fein and Walther (1987) indicate that calcite solubility in CO_2-H_2O solutions should remain vanishingly small at elevated *P*-*T* conditions. The great carbonate transport and metasomatism at near-granulite-grade *P*-*T* conditions, as described by Dahlgren et al. (1993) in the Bamble region, is difficult to explain unless some additional factors operate to counteract the effects of high temperature and low H_2O activity.

Concentrated NaCl solutions have the property of very low H_2O activity at pressures above 4 kbar at elevated temperatures (Aranovich and Newton 1996; Shmulovich and Graham 1996), and hence deserve consideration as feasible metamorphic fluids (Newton et al. 1998). Moreover, primary fluid inclusions in some rocks of deep-seated origin, such as the eclogite veins in the Western Alps described by Philippot and Selverstone (1991), contain extremely concentrated brines with daughter crystals of calcite and dolomite, as well as anhydrite, barite, monazite, and other trace-element-rich minor minerals. These features suggest that concentrated brines may be powerful solvents at elevated *P*-*T* conditions for carbonates and other non-silicate oxysalt minerals.

NaCl induces a large enhancement of calcite solubility at very low temperatures and pressures, similar to the effect of CO_2 at these conditions (Ellis 1963). Fein and Walther (1989) found a significant NaCl enhancement of calcite solubility at supercritical conditions of 600 °C and 2 kbar; however, the maximum salinity that they investigated was 0.02 molal. At higher NaCl concentrations, it might be anticipated that calcite solubility should decrease with decreasing H_2O activity, as in the CO_2-H_2O system. The effect of NaCl on calcite solubility at higher *P*-*T* conditions, where the solute properties of NaCl change from those of an undissociated neutral complex to a completely ionized solution (Aranovich and Newton 1996), has not been investigated. The present study was designed to measure calcite solubility at elevated *P*-*T* conditions in NaCl solutions sufficiently concentrated to have the low H_2O activity suitable for deep crustal-upper mantle metamorphic fluids.

Experimental methods

Solubility experiments were carried out by reacting a very pure natural calcite with H_2O of variable NaCl content from pure H_2O to halite saturation in sealed Pt envelopes in the internally heated piston-cylinder apparatus with NaCl pressure medium and graphite heater sleeves. Pressures were 6 to 14 kbar at 700 °C, and temperatures were 600 to 900 °C at 10 kbar. The experimental procedures were identical to those of Newton and Manning (2000) except that the calcite crystals in most of the present experiments were encapsulated in a small inner Pt container that was perforated with numerous pinholes to allow access of the salt solution from the outer capsule. This procedure was necessary because the starting calcite cleavage chips usually recrystallized to an aggregate of rounded crystals, which required containment. Pressures are accurate to ±300 bars and automatically controlled temperatures, measured by calibrated matched pairs of W3%Rh-W25%Rh thermocouples, are accurate to ±3 °C.

Clear cleavage rhombs of calcite from Rodeo, Durango, Mexico, were used. Microprobe analysis showed that the maximum departure from $CaCO_3$ composition was 0.07 wt% FeO (Caciagli 2001). Reagent-grade NaCl and distilled and deionized water completed the starting materials. Ingredients were successively weighed into the outer Pt capsule on a Mettler M3 microbalance with $1\sigma = 0.002$ mg. H_2O content was checked after an experiment by puncturing and drying the outer capsule at 310 °C for 15 minutes ("H_2O out" in Table 1). Calcite solubility values were determined by weighing the inner Pt capsules before and after each experiment. Inner Pt capsules retrieved from an experiment were soaked in warm H_2O to dissolve away precipitated salt inside the capsule. A series of 5 to 8 ten-minute soakings, followed by dryings at 115 °C and reweighings were performed until a capsule came to constant weight. Because of the high calcite solubilities encountered at run conditions, a significant portion of H_2O-insoluble quench calcite remained in the inner capsules; therefore, the solubility determined by weight loss of the inner capsule was a minimum value. The Pt capsule was cut open with a razor blade and the calcite charge was transferred quantitatively to a Pt weighing pan. The quenched "fuzz" of skeletal calcite crystals was clearly distinguishable from the rounded undissolved crystals. It was possible to remove most of the fuzz with a needle under a binocular microscope, but it proved impossible to accomplish this cleaning process without the loss of a small amount of granular calcite. The weight of the cleaned residual crystals thus provided an upper limit for calcite solubility.

RESULTS

Experimental results are given in Table 1. The 1σ errors associated with each weighing step were propagated to establish uncertainties in the solubility limits and X_{NaCl} [$X_{NaCl} = n_{NaCl}/(n_{NaCl} + n_{CaCO_3} + n_{H_2O})$, where n is number of moles of the subscripted compound in the fluid]. Equilibrium calcite saturation of the fluids is demonstrated by time-independence of the measured solubilities at 700 °C and 10 kbar with a NaCl mole fraction near 0.15 and at 600 °C with NaCl mole fraction near 0.30 (Table 1). Recrystallization of the original cleavage rhombs into aggregates of solution-rounded and solution-polished crystals (Fig. 1a), is another indication that calcite-solution equilibrium was closely approached.

Figure 1b shows a portion of the dried, quenched vapor-phase. Skeletal quench-calcite crystals outline rhomb-shaped cells filled by halite in experiments with high NaCl (and solute $CaCO_3$). This texture indicates that skeletal calcite precipitated first in the quench, forming a rhomb-shaped framework that constrained subsequently precipitated halite. Semi-quantitative energy-dispersive analysis of the skeletal calcite crystals showed no Na or Cl, and the halite was Ca-free.

An experiment at 900 °C and 10 kbar with pure H_2O yielded an opaque bead of calcite (Fig. 1c), rather than the limpid, rounded aggregates encountered at lower temperatures. Surface textures of the bead were similar to those described by Wyllie and Tuttle (1960) in experiments on the join $CaCO_3$-H_2O at 1 kbar, >750 °C, in which melting was inferred. Our experiments do not define closely the hydrous solidus at 10

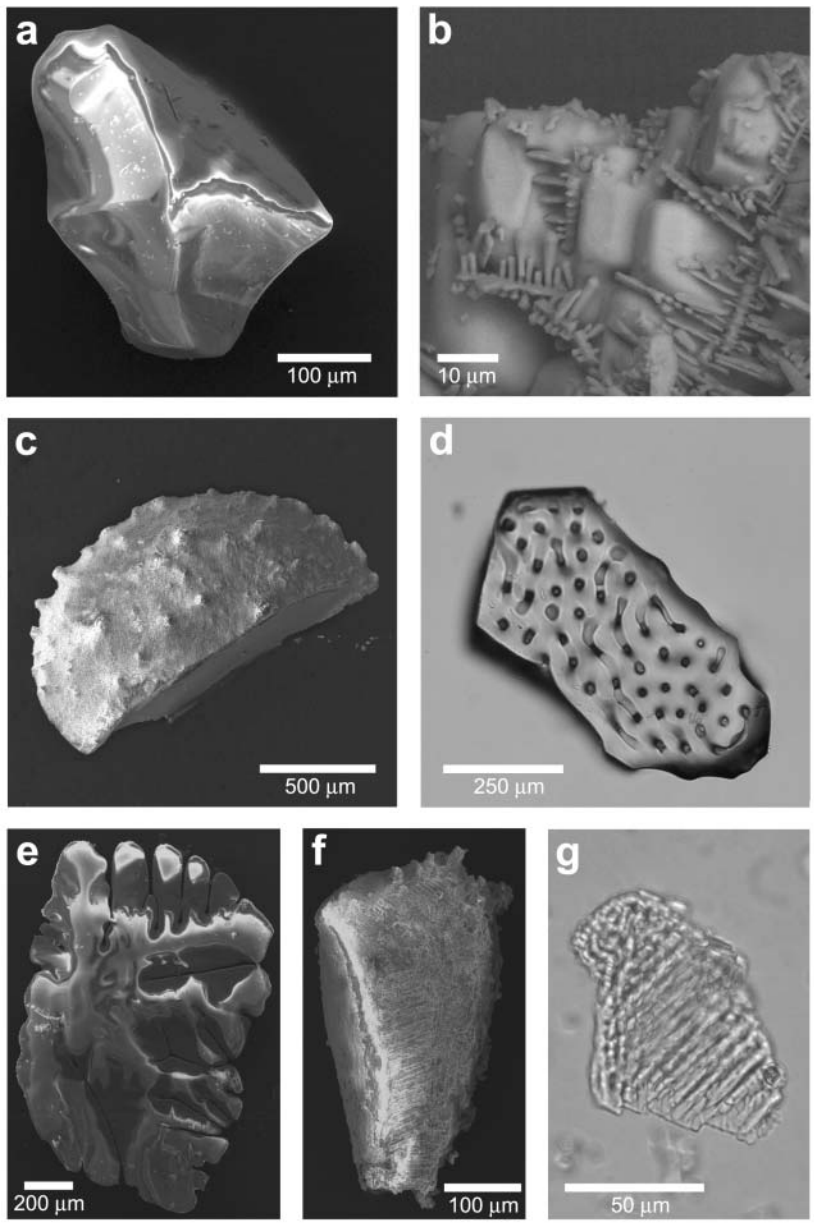

FIGURE 1. Scanning electron microscope (SEM) images and photomicrographs of synthesis products of selected experiments. (**A**) Recrystallized calcite aggregate from run no. 28 (Table 1), 800 °C, 10 kbar, $X_{NaCl} = 0.38$. Secondary electrons. (**B**) SEM image of intergrown skeletal quench calcite and rounded quench halite, run no. 14 (Table 1), 800 °C, 10 kbar, $X_{NaCl} = 0.53$. The rhomb-shaped aspect of some of the halite crystals suggests that the calcite precipitated first in the quench, forming rhombohedral matrices which constrained the shape of the subsequently precipitated halite. Secondary electrons. (**C**) Bead of former carbonate liquid, quenched to calcite, run no. 31 (Table 1), 900 °C, 10 kbar, initially pure H_2O. The lower sides of the bead conform to the shape of the capsule during the experiment. The surface protuberances represent calcite growth during quench. Secondary electrons. (**D**) Photomicrograph of calcite crystal grown at 900 °C, 10 kbar, $X_{NaCl} = 0.30$ (run no. 30, Table 1). Arrays of regularly spaced fluid inclusions, originally halite, carbonate, brine, and vapor, are mostly decrepitated. Ordinary light, immersion oil ($n = 1.48$). (E) SEM image of flat, lobate single calcite crystal, run no. 36 (Table 1), 900 °C, 10 kbar, $X_{NaCl} = 0.20$. The crystal coexisted with carbonate-rich liquid + saline aqueous fluid. Secondary electrons. (**F**) Porcelainous bead interpreted to be quenched to calcite from carbonate-rich liquid, run no. 36 (Table 1), 900 °C, 10 kbar, $X_{NaCl} = 0.20$. The liquid coexisted with calcite + saline aqueous fluid. Secondary electrons. (**G**) Photomicrograph of lightly crushed bead of quenched carbonate liquid which coexisted with flat calcite crystal in run no. 36 (Table 1), 900 °C, 10 kbar, $X_{NaCl} = 0.20$. The barred skeletal crystals of the crushed bead are texturally distinct from the fibrous skeletal calcite crystallized from the vapor phase during the quench. Ordinary light, immersion oil ($n = 1.48$).

TABLE 1. Experimental results

Expt. number	Temperature (°C)	Pressure (kbar)	Duration (h)	NaCl in (mg)	H_2O in (mg)	H_2O out (mg)	Capsule in (mg)	Capsule out (mg)	Calcite in (mg)	Calcite out (mg)
4	600	10	71	0.000	22.315	22.335	65.906	65.867	0.666	0.616
26	600	10	132	17.585	25.481	25.387	64.174	63.904	2.538	2.155
2	600	10	85	15.094	11.058	11.165	47.808	47.566	0.687	0.369
3	600	10	47	16.202	11.062	11.133	37.202	36.959	0.378	0.119
34	700	6	71	28.136	19.885	19.958	65.611	64.726	1.608	0.669
20	700	10	69	0.000	22.328	22.364	48.312	48.187	0.930	0.678
16	700	10	147	6.037	10.632	10.289	60.574	60.327	0.801	0.524
25	700	10	85	16.140	25.331	24.874	50.766	50.228	1.420	0.802
15	700	10	89	13.712	11.202	10.841	60.861	60.400	1.489	0.940
27	700	10	64	43.695	21.126	21.417	66.093	64.657	1.553	0.077
35	700	14	46	27.596	19.979	20.010	61.177	60.088	3.311	2.175
19	800	10	10	0.000	5.621	5.649	52.688	52.674	0.911	0.845
22	800	10	79	3.219	22.210	22.159	63.032	62.695	1.120	0.780
10	800	10	6	8.238	22.128	22.807*	57.003	56.365	0.708	0.000
9	800	10	68	8.980	18.037	19.491*	61.853	61.167	1.313	0.551
13	800	10	86	17.748	18.116	17.687	71.897	70.595	2.078	0.692
7	800	10	47	14.513	11.156	10.854	70.096	69.051	3.116	1.886
5	800	10	48	19.428	11.331	10.447	71.624	70.158	1.520	0.000
28	800	10	61	22.484	11.065	11.116	71.586	69.896	3.036	1.219
11	800	10	96	21.452	8.674	8.613	76.571	74.785	3.799	1.800
21	800	10	46	18.581	7.060	6.843	68.143	66.774	3.582	1.920
24	800	10	64	17.110	5.806	5.740	64.452	62.993	2.756	1.203
14	800	10	68	18.435	5.834	4.975	68.800	67.225	3.196	1.512
12	800	10	91	22.825	5.890	5.914	85.652	83.707	5.834	3.698
31	900	10	9	0.000	24.912	25.113	–	–	1.148	–
36	900	10	12	15.379	19.248	19.383	–	–	3.333	0.480
32	900	10	20	16.893	20.626	20.489	–	–	2.304	0.000
37	900	10	13	16.572	20.125	19.902	–	–	2.474	0.000
30	900	10	12	20.826	14.859	14.810	–	–	5.542	0.960
29	900	10	17	23.503	16.747	16.684	–	–	4.127	0.000
33	900	10	15	22.578	15.828	15.850	–	–	4.539	0.000

Notes: "In" and "out" refer respectively to weights before and after experiment. Mass of H_2O out was used in all calculations (see text), except where marked by asterisk. In these cases, initial mass of H_2O was used because some solution was lost as spray during capsule opening. At ≤ 800 °C, minimum calcite solubility was calculated by loss in weight of capsule + crystals, which includes minor quench crystals; maximum solubility was determined by extracting crystals from capsule and removing quench material, which usually included a few grains of non-quench calcite. At 900 °C, no inner capsules were used (see text), so solubility was determined from crystal weights. Parenthetical numbers are 1σ uncertainty in last digit, propagated from weighing errors; the small errors in X_{NaCl} (<2.3×10^{-4}) are ignored.

kbar in the system CaO-H_2O-CO_2, but they show that major amounts of liquid are generated between 800 and 900 °C in NaCl-absent experiments.

Figure 2 shows the experimental solubility brackets at 10 kbar defined from maximum and minimum weight changes as described in the preceding section. Brackets of calcite solubility at 900 °C and 10 kbar were obtained with unencapsulated rhombs by simply noting the presence or absence of coarse-grained calcite in the quenched charges. The brackets could be tightened somewhat by retrieving and weighing calcite crystals that were inferred from texture to be primary. The primary calcite formed a thin flat layer at the bottom of the capsule in an experiment with $X_{NaCl} = 0.302$ (run no. 30, Table 1). It was composed of a flat single crystal with arrays of regularly spaced fluid inclusions, mostly decrepitated in the drying process (Fig. 1d). The fluid inclusions probably formed by necking down of fluid-filled tubes or films trapped at former grain boundaries by recrystallization. A few intact inclusions contained a large halite crystal, smaller birefringent crystals, and a vapor bubble. The arrays of fluid inclusions are consistent with the presence of crystalline calcite at experimental conditions. An experiment at 900 °C, 10 kbar, $X_{NaCl} = 0.197$ (run no. 36, Table 1), yielded a few large flat lobate calcite crystals (Fig. 1e) that coexisted with several porcelainous beads (Fig. 1f) tentatively inferred to be quenched carbonate liquid. One of these beads was crushed under immersion oil. It disaggregated to a mass of flat, barred, skeletal crystals (Fig. 1g), possibly indicative of a quenched carbonate melt. The solidus at 900 °C and 10 kbar is therefore provisionally inferred to lie close to 20% NaCl.

DISCUSSION

P-T-X$_{NaCl}$ dependence of calcite solubility

Figure 2 illustrates that there is a great enhancement of calcite solubility with increasing temperature and salinity of the fluid. At 800 °C and 10 kbar, the most saline fluids obtainable (slightly halite undersaturated) can dissolve $CaCO_3$ to concentrations of nearly 4 molal, corresponding to 6 wt% of the solution, or one quarter the weight of the water. Our precision is not sufficient to measure accurately the solubility in pure H_2O at these conditions, but extrapolation from high salinity shows that the concentration is about 0.1 molal, consistent with the results of Caciagli (2001). The possible enhancement in NaCl solutions relative to pure H_2O at 800 °C and 10 kbar is thus about 40 times. A great decrease in solubility at a given NaCl mole fraction occurs between 900 and 600 °C at 10 kbar. At 600 °C, halite saturation occurs when the $CaCO_3$ molality is only 0.25. The pressure effect on solubility is much smaller than the temperature effect: at 700 °C and $X_{NaCl} = 0.3$, the $CaCO_3$ solubility increases only about 20% between 6 and 14 kbar (Table 1).

The distribution of the 800 °C solubility data suggests a power-law dependence of calcite solubility on NaCl mole frac-

TABLE 1. —*Extended*

X_{NaCl} in	Minimum solubility (molal)	Maximum solubility (molal)	Notes
0.000	0.017(1)	0.022(1)	
0.176	0.106(1)	0.151(1)	
0.294	0.217(3)	0.285(2)	
0.310	0.218(3)	0.233(2)	
0.303	0.443(1)	0.470(1)	
0.000	0.056(1)	0.113(1)	
0.153	0.240(3)	0.269(2)	
0.167	0.216(1)	0.248(1)	
0.281	0.425(3)	0.506(2)	
0.386	0.670(1)	0.689(1)	
0.298	0.544(1)	0.568(1)	
0.000	0.025(5)	0.117(1)	
0.043	0.152(1)	0.153(1)	
0.103	0.320(1)	–	
0.133	0.380(2)	0.422(1)	
0.236	0.736(2)	0.783(2)	
0.292	0.963(3)	1.133(2)	
0.364	1.455(3)	–	
0.384	1.520(3)	1.634(2)	
0.434	2.073(3)	2.320(3)	
0.456	2.000(4)	2.428(3)	
0.479	2.541(5)	2.705(5)	
0.533	3.165(6)	3.384(5)	
0.543	3.288(5)	3.611(4)	
0.000	–	–	melted
0.197	–	1.472(1)	possible melt
0.203	1.124(1)	–	possible melt
0.204	1.243(1)	–	possible melt
0.302	–	3.093(2)	
0.303	2.473(1)	–	
0.305	2.863(1)	–	

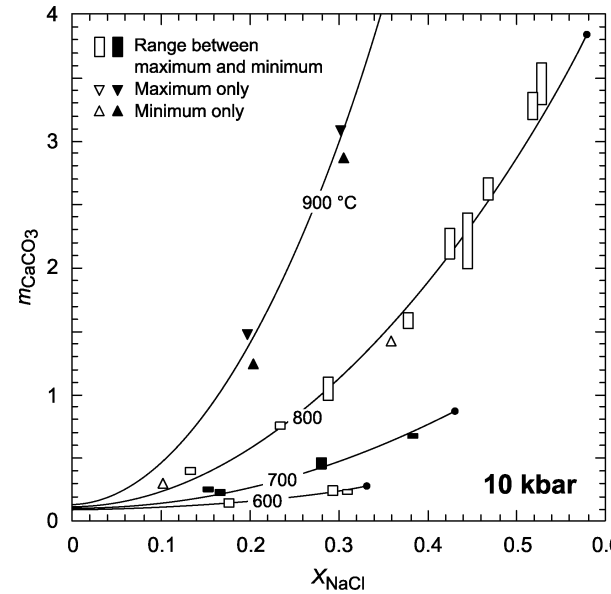

FIGURE 2. Experimentally determined $CaCO_3$ molality (moles $CaCO_3$ dissolved per kg H_2O) at 10 kbar, as a function of X_{NaCl} [$X_{NaCl} = n_{NaCl}/(n_{NaCl} + n_{CaCO_3} + n_{H_2O})$, where *n* is number of moles of the subscripted compound in the fluid]. Vertical dimensions of rectangles correspond to the range between maximum and minimum solubility from a single experiment (see text). Triangles represent experiments that constrain only maximum or minimum solubility. Only the most constraining experiments are shown at 900 °C. Isothermal curves are based on regression of the 700, 800, and 900 °C brackets (Eq. 3, text); portions at >800 °C are metastable with respect to melt (Table 1). The 600, 700, and 800 °C curves are extrapolated to the X_{NaCl} values of halite saturation (filled circles) in the system NaCl-H_2O (Aranovich and Newton 1996), ignoring dissolved $CaCO_3$.

tion (Fig. 2). Figure 3 shows that the NaCl molality is linear with the square of the NaCl mole fraction. Least-squares regression of the bracket midpoints at 800 °C, 10 kbar, gives:

$$m_{CaCO_3} = 0.096 + 11.562X^2_{NaCl} \quad (1)$$

for which the correlation coefficient is 0.997. The intercept of 0.096 *m* in pure H_2O is quite close to the value of 0.081 ±0.042 measured by Caciagli (2001). The high correlation coefficient indicates that Equation 1 is useful as a simple expression for prediction of calcite solubility over a wide range of X_{NaCl}; however, it is not meant to imply that the same set of aqueous species predominates over this range of fluid composition. For example, Fein and Walther (1989) noted that Ca^{2+} predominated at low X_{NaCl}, but $CaCl^+$ became the dominant Ca species as X_{NaCl} increased at 2 kbar, 400–600 °C. The departure of our two measurements from the linear trend in Figure 3 at very dilute NaCl concentrations may reflect such changes in the predominance of aqueous species. The fewer data at 600 and 700 °C can be fitted less precisely to similar isothermal quadratic functions.

The temperature dependence of $CaCO_3$ molality at constant *P* and X_{NaCl} was found to be fit well by a function of the form:

$$\log m_{CaCO_3} = C_1 + C_2T^2 \quad (2)$$

A general calcite solubility formula was derived by regression of the isothermal parameters, combined with the measured pressure dependence at 700 °C, assumed to apply as a constant proportion of the solubility:

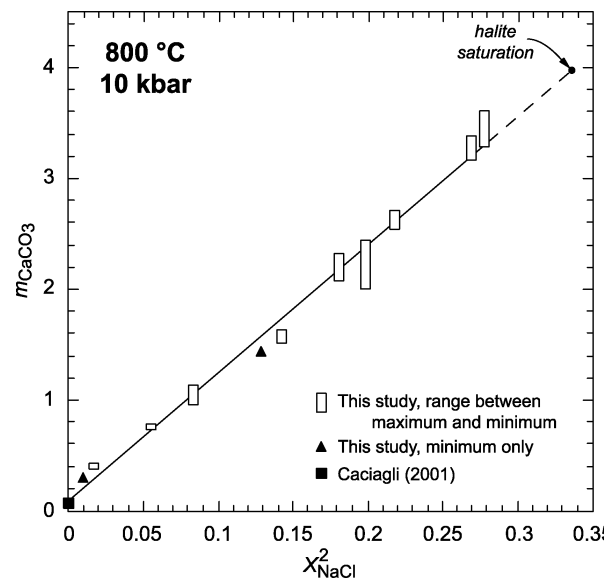

FIGURE 3. Experimental brackets of $CaCO_3$ at 800 °C, 10 kbar, vs. the square of the NaCl mole fraction (including solute $CaCO_3$ content). Linear regression of the bracket midpoints gives the relation of Equation 1, text, with r = 0.997.

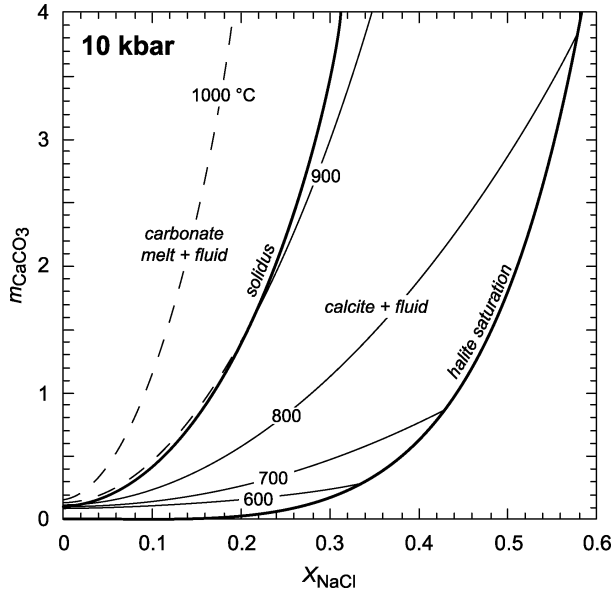

FIGURE 4. Interpretive phase relations in the system $CaCO_3$-H_2O-NaCl at 10 kbar in terms of X_{NaCl} and $CaCO_3$ molality. Bold lines are univariant three-phase curves; light solid lines are calcite solubility isotherms (dashed where metastable with respect to melt).

$$m_{\mathbf{CaCO_3}} = [-0.051 + 1.65 \times 10^{-4}\, T + X_{NaCl}^2 \exp(-3.071 + 4.749 \times 10^{-6} T^2)]\ (0.76 + 0.024P) \quad (3)$$

with *T* in Kelvins and *P* in kbar. The 600 °C data were not included in the regression because the small solubilities exert undo influence on the overall fit. Isothermal curves given by Equation 3 are shown in Figure 1. It can be seen that the extrapolated 600 °C curve satisfies the experimental data at that temperature. One standard deviation in the difference between experimental midpoints and solubility calculated from Equation 3 corresponds to 6% relative.

The 10 kbar results were used to generate an interpretive isobaric phase diagram for the system $CaCO_3$-H_2O-NaCl (Fig. 4). The isobarically univariant solidus and halite-saturation curves define two divariant *T*-*X* fields: a high-*T*, two-liquid field (brine + hydrous carbonate melt), and a calcite + fluid field. For bulk compositions with X_{NaCl} greater than halite saturation, the fluid composition coexisting with calcite and halite lies on the halite saturation curve. Isopleths of calcite solubility (Eq. 3) are only stable in the calcite + fluid field. Predicted metastable calcite solubility above the solidus, shown with dashed lines, crudely approximates the melt solubility. The proposed similarity in the geometry of the solidus and the 900 °C solubility isopleth, along with the very steep rise in the 1000 °C extrapolated curve with salinity, imply critical mixing between salt solutions and carbonate liquids at ~1000 °C and X_{NaCl} perhaps no higher than 0.3.

Solution mechanism

The great increase of $CaCO_3$ solubility with salinity at constant *P* and *T* implies the existence of a solution reaction involving NaCl. The accelerating trend shows that H_2O is not involved in the reaction; if it were, the rapidly decreasing H_2O activity with NaCl mole fraction at 10 kbar would inhibit calcite solubility in concentrated solutions. It follows that HCO_3^- is not a significant species in concentrated NaCl solutions at high temperatures and temperatures. Thus calcite-solution equilibrium can be described by:

$$\underset{\text{calcite}}{CaCO_3} + 2NaCl_{aq} = CaCl_{2,aq} + Na_2CO_{3,aq} \quad (4)$$

Regardless of the extent of dissociation of the aqueous species, Equation 4 shows that one mole of calcite dissolves to two moles of solute products. As the activity of NaCl is approximately equal to the square of its mole fraction (Aranovich and Newton 1996), the result is that the $CaCO_3$ molality is approximately proportional to the square of the NaCl mole fraction. The dominant Ca solute species in concentrated NaCl solutions is probably $CaCl^+$ (Fein and Walther 1989), and $NaCO_3^-$ would be the most likely saline carbonate species.

Aranovich and Newton (1996) noted that concentrated NaCl-H_2O solutions at pressures higher than about 5 kbar behave more like fused salts than aqueous solutions in their thermodynamic mixing properties. This model is reinforced by the solution behavior of $CaCO_3$: reaction 4 and Equation 1 imply that the solute speciation is that of an ideal fused salt, in which the activities of all solute species, including molecular H_2O, closely approach their molecular concentrations (Bradley 1962). If the $CaCO_3$ mole fraction at calcite saturation is extrapolated to the NaCl-$CaCO_3$ join (Fig. 5), the result is a metastable binary halite-calcite eutectic composition of about 5.8 mol% $CaCO_3$. The one-bar eutectic composition found by Niggli (1919) is about 3 mol% $CaCO_3$. His eutectic temperature is 789 °C. The small difference in eutectic composition is explained by the 11 °C temperature difference and by the 10 kbar pressure shift. Adjustment of the value of Figure 5 to 1 bar and 789 °C by Equation 3 gives an estimated eutectic composition of 3.6 mol% $CaCO_3$.

The ideal fused-salt model may provide insights into the general solution behavior of non-silicate oxysalt minerals in concentrated brines at elevated temperature and pressure. An ionic solid may be expected to undergo a salting-in reaction at pressures of several kbar analogous to Reaction 4 provided that the reaction products are reasonably soluble. The solute concentrations as a function of NaCl (or KCl) mole fraction may be predicted approximately if the ionic solid exhibits an anhydrous fused-salt eutectic like the NaCl-$CaCO_3$ binary. Compounds that may dissolve in concentrated brines in a manner analogous to calcite may include sulfates, borates, and phosphates.

Geologic applications

Metasomatic processes. The problem of huge carbonated terranes is greatly ameliorated by the solubility enhancement of calcite in solutions of even moderate salinity at high-grade metamorphic conditions. At 900 °C and 10 kbar, calcite solubility is enhanced by a factor of 20 in a solution of 30 mol% NaCl over the solubility in pure H_2O. Such a solution would

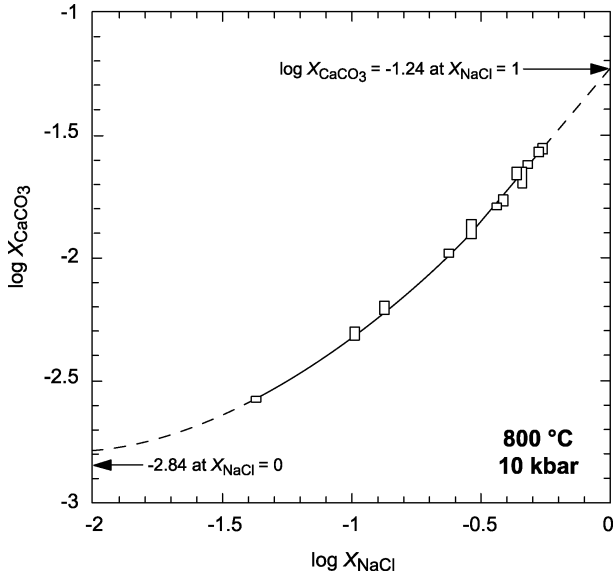

FIGURE 5. Logarithmic extrapolation of $CaCO_3$ solubility, expressed as mole fraction, in concentrated NaCl solutions at 10 kbar and 800 °C. Linear regression of the eight highest-NaCl bracket-midpoints gives an extrapolated, metastable eutectectic composition on the NaCl-$CaCO_3$ binary of 5.6% $CaCO_3$, compared to about 3% at 1 bar, 789 °C (Niggli 1919).

have low enough H_2O activity to traverse the middle crust without provoking extensive hydration or melting (Aranovich and Newton 1998). If initially saturated with calcite, the solution would lose 85% of its solute $CaCO_3$ upon cooling only 200 °C. Halite saturation would be deferred to temperatures well below 500 °C if the pressure decreases concomitantly to ~4 kbar, especially if Na is lost in scapolite- or albite-forming reactions such as described in the Mary Kathleen Fold Belt by DeJong and Williams (1995). The drastic decrease of calcite solubility in cooling of concentrated salt solutions between 900 and 600 °C appears adequate to explain the great accumulation of metasomatic carbonate in the megashear zones.

The high solubility of calcite and, undoubtedly, other carbonates, in concentrated salt solutions at elevated *P-T* conditions implies that concentrated brines, if present in the deep crust and upper mantle, are not likely to be merely alkali chloride solutions, but may often acquire a substantial solute load of carbonate, whatever their origin. Scavenging of carbonate by hypersaline solutions may be especially important where such solutions traverse metasedimentary sequences. Various carbonates have been identified as daughter minerals in concentrated brine inclusions in eclogite veins from the Western Alps (Philippot and Selverstone 1991; Scambelluri et al. 1998), and associated with the chloride-carbonate brines trapped in cloudy diamonds in xenoliths from South African kimberlite pipes (Izraeli et al. 2001). The carbonate component of ascending deep-crust and upper mantle solutions will become susceptible to decarbonation reactions with silicate minerals and quartz as pressure is reduced. This mechanism could give rise to the associated suites of CO_2-rich fluid inclusions that have been observed with brine inclusions in granulites (Touret 1985; Crawford and Hollister 1986; Herms and Schenk 1998). Extraction of H_2O by hydration reactions, as in the amphibole-forming reactions in the Lofoten, Norway granulites described by Markl and Bucher (1998), will concentrate brine components of grain-boundary fluids, eventually leading to salt precipitation, as reported by these authors. Alkali exchange between brines and feldspars, as in albitization, metasomatic antiperthite (Franz and Harlov 1998), and myrmekite formation, will affect alkali ratios and may either supply Ca to, or deplete Ca in, the complex brines. Thus, the fluid-rock processes involved in migrating salt solutions in the deep crust or upper mantle are likely to be quite complex.

Anhydrite, $CaSO_4$, is quite insoluble in pure H_2O, but is likely to be more soluble in concentrated brines. The 1 bar $CaSO_4$-NaCl join shows a profound eutectic at 721 °C and nearly 37 wt% $CaSO_4$ (Bergman and Golubeva 1953). Moreover, $CaCl_2$ and Na_2SO_4, the postulated salting-in reaction products, are very soluble in H_2O. By analogy with calcite, anhydrite is predicted to show large salting-in with concentrated NaCl solutions at high-grade metamorphic conditions. A major effect on rock interaction with sulfate-rich brines may be to produce extremely oxidizing fluids when S^{6+} from dissolved sulfate encounters Fe-oxides or Fe-silicates and reacts to form pyrrhotite with S^{2-}, as postulated for South Indian granulites by Harlov et al. (1997). In addition, Carmichael (1991) found high intrinsic oxidation states in alkali basalts on the basis of their Fe^{3+}/Fe^{2+} ratios, commonly near hematite stability. Evolution of a saline fluid phase on crystallization of alkaline magmas, as advocated by Hansteen and Burke (1990), could be a potent source of highly oxidizing fluids capable of transporting significant $CaSO_4$.

The phosphate minerals apatite and monazite may, by analogy with calcite, show enhanced solubility in concentrated brines, inasmuch as Na phosphate is highly soluble. Apatite is an abundant and almost ubiquitous accessory mineral in crustal rocks and is the most important carrier of the rare-earth elements. Monazite is one of the most important reservoirs of Th and U in rocks and is correspondingly important in heat-flow and geochronology considerations. Dissolution and reprecipitation of these minerals by migrating brines could be important factors in geochemical segregation processes and economic mineral concentration in the crust. Swarms of granulite-facies alteration veins in Namaqualand, South Africa (Andreoli et al. 1993) have such high monazite concentrations that they constitute significant ore bodies. The distribution of monazite in the Sharyzhalgay charnockites of Siberia cannot be explained by magmatic processes, but requires transport by migrating solutions (Nozhkin and Turkina 1995). The solutions involved in both of these occurrences were most probably highly saline. Monazite has been reported as a daughter mineral in hypersaline fluid inclusions in eclogite veins in the western Alps (Philippot and Selverstone, 1991). Apatite is a common metasomatic mineral along with calcite in the fenite aureoles of the Alnö complex, Sweden (Morogan and Woolley 1988).

Possible mantle origin of carbonate-rich saline solutions. Most of the authors who have described the large-scale linear zones of carbonate alteration have concluded, on the basis of

mantle-like C- and Sr-isotope ratios, that the fluids which deposited the carbonates were initially of mantle origin (Baratov et al. 1984; Lapin and Ploshko 1988; Stern and Gwinn 1990; Oliver et al. 1993; Dahlgren et al. 1993; Wickham et al. 1994). The associations with small bodies of alkaline igneous rocks in the South Tien Shan and Attur Valley occurrences, as well as with small bodies of probable igneous carbonatite in the Attur Valley (containing olivine, diopside, and phlogopite), suggests strongly that the carbonate megashear zones were conduits of mantle-derived volatiles during episodes of lithospheric reactivation. Wickham et al. (1994) regarded the fluids as nearly juvenile magmatic emanations, with only a small imprint of the Precambrian crust that they traversed. Baratov et al. (1984), on the other hand, doubted that the metasomatizing fluids were largely derived from crystallization of the associated alkali basalt dikes, because of the much smaller exposures of the latter, but consider probable a common mantle origin of both fluids and basalt magmas. None of the above authors make a causal connection between hypersaline fluids and carbonate metasomatism. Oliver et al. (1993) attach importance to the great amount of alkali metasomatism of the surrounding rocks, and infer that metasomatizing fluids were highly saline, but consider that the salt content of the fluids was derived from evaporite sequences invaded by the carbonate bodies. Lapin et al. (1987) do not attempt to link genetically the alkaline metasomatites with the linear carbonate bodies in the Tatar Fault zone other than to note their ubiquitous association. A more direct association of alkaline metasomatism with vapor-transported carbonate is the fenite aureole of the Alnö alkaline complex (Morogan and Woolley 1988).

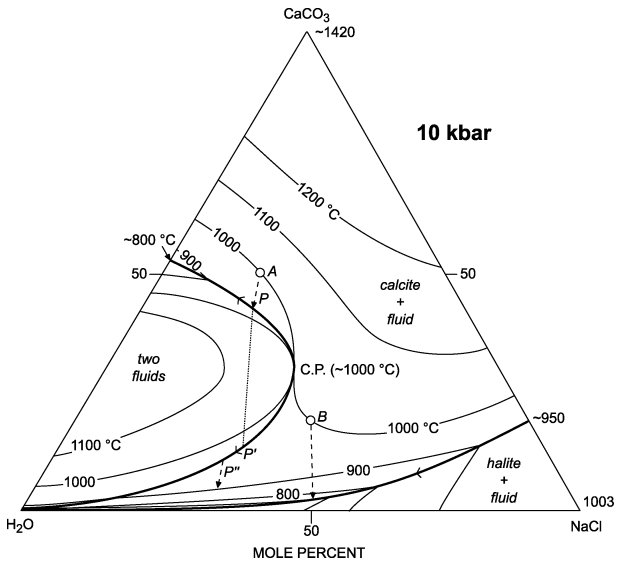

FIGURE 6. Semi-schematic phase equilibrium diagram of the pseudo-ternary system $CaCO_3$-NaCl-H_2O at 10 kbar based on the present study and Niggli (1919), Clark (1959), Wyllie and Tuttle (1960), Irving and Wyllie (1981), Koster Van Groos (1991), and Caciagli (2001). Critical mixing between a hydrous, NaCl-bearing carbonatite liquid and a $CaCO_3$-rich hypersaline aqueous solution is suggested to occur near 1000 °C and 30% NaCl, 25 mol% $CaCO_3$.

The present work, together with the observed phenomena of carbonate deposition in the carbonated megashear zones, is consistent with high-temperature precipitation of the carbonates from hypersaline fluids, formed either as late-magmatic emanations from alkalic basalts in the deep crust, or formed simultaneously with alkalic magmas in tectonic/thermal activation of the mantle in deep fault zones. The fluids invaded the crust at near-magmatic temperatures and deposited their carbonate load upon cooling only a few hundred degrees. It may well have happened that a CO_2-rich fluid became immiscible with the saline fluid during or after separation from the mantle or from mantle-derived magmas. At mid-crustal levels, much of the solute carbonate would be lost in alkali metasomatism because some possible metasomatic reactions must also be decarbonation reactions. It might sometimes be necessary for the conduits to become armored with alkaline metasomatites before actual carbonate deposition occurs. This interpretation would be consistent with the spatial distribution of carbonate bodies and their metasomatic haloes in the Tatar Deep Fault zone (Lapin et al. 1987). In other cases, as in the Attur Valley, whole-rock replacement of granulite gneisses by carbonate has occurred.

The experimental results suggest a possible link between igneous carbonatite and carbonate-metasomatizing aqueous fluids, as in the Attur Valley. The relations are suggested by the semi-schematic diagram of Figure 6, which is consistent with available information for the pseudo-ternary system at 10 kbar. A supercritical fluid at 1000 °C, initially saturated with $CaCO_3$ and with relatively low NaCl content (a mantle-derived or exhalative carbonate-rich liquid represented by point A) would, upon cooling and precipitating calcite, split into two fluids at a temperature near 950 °C (points P and P'). One of these fluids (P), a carbonatite liquid, would become slightly more carbonate-rich with decreasing temperature over a short interval, and the other (P^1), an aqueous solution, would become less carbonate-rich and progressively less saline with decreasing temperature until the coexisting liquid is entirely consumed. The remaining concentrated brine at point P" would then begin to precipitate calcite exclusively with further cooling. Fluids that are initially less carbonate-rich and more saline (point B), would avoid the two-fluid field in cooling, and eventually encounter halite saturation at much lower temperatures. The great bulk of the solute carbonate would be precipitated in cooling from near-magmatic to middle-grade temperatures. A reaction with crustal rocks that removes NaCl, as in scapolite formation, would hasten the carbonate deposition process. Examples of fault-zone scapolite are the Cloncurry Fault Zone (Edwards and Baker 1953) and the Melones Fault Zone (Albino 1995). An important problem to be investigated experimentally is the NaCl/$CaCO_3$/$CaSO_4$ content of scapolite formed by reaction of high *P*-*T* saline fluids with feldspars as a function of solute concentrations and physical conditions, building on the work of Ellis (1978). The role of F in such solutions, especially where metasomatism is associated with carbonatites and alkalic igneous rocks, is another important experimental dimension indicated by carbonatite complexes and their metasomatic aureoles (Gittens et al. 1990).

ACKNOWLEDGMENTS

This research was supported by National Science Foundation grant EAR-9909583 to C.E.M. We thank James Brenan, Colin Graham, and Zach Sharp for helpful reviews. Casey Donahue provided the electron microprobe analysis of the calcite. Natalie Caciagli and George Jarzebinski assisted with the SEM work. Wayne Dollase helped with X-ray diffraction studies. Several preliminary experiments in this system were done by Benjamin Newton.

REFERENCES CITED

Albino, G.V. (1995) Sodium metasomatism along the Melones Fault Zone, Sierra Nevada Foothills, California. Mineralogical Magazine, 59, 383–400.

Andreoli, M.A.G., Smith, C.B., Watkeys, M., Moore, J.M., Ashwal, L.D., and Hart, A.R.G. (1993) Th-REE-U enriched charnockites of Namaqualand, South Africa: implications for granulite petrogenesis. Geocongress '92 Extended Abstracts, 1–3. Geological Society of South Africa, Bloenfontein, South Africa.

Aranovich, L.Y. and Newton, R.C. (1996) H_2O activity in concentrated NaCl solutions at high pressures and temperatures measured by the brucite-periclase equilibrium. Contributions to Mineralogy and Petrology, 125, 200–212.

———(1998) Reversed determination of the reaction: phlogopite + quartz = enstatite + K-feldspar + H_2O in the ranges 750–875 °C and 2–12 kbar at low H_2O activities with concentrated KCl solutions. American Mineralogist, 83, 193–204.

———(1999) Experimental determination of CO_2-H_2O activity-composition relations at 600–1000 °C and 6–14 kbar by reversed decarbonation and dehydration reactions. American Mineralogist, 84, 1319–1332.

Baratov, R.B., Gnutenko, N.A., and Kuzemko, V.N. (1984) Regional carbonization connected with the epi-hercynian tectogenesis in the southern Tien Shan. Doklady Akademiia Nauk S. S. R., 274, 124–126.

Bebout, G.E. and Barton, M.D. (1989) Fluid flow and metasomatism in a subduction zone hydrothermal system: Catalina Schist terrane, California. Geology, 17, 976–980.

Bergman, A.G. and Golubeva, M.S. (1953) Complex formation of the double heteroionic salt type (anhydrous kainites) in ternary reciprocal systems. Doklady Akademiia Nauk S. S. R., 89, 471–473.

Bradley, R.S. (1962) Thermodynamic calculations on phase equilibrium involving fused salts. Part I. General theory and application to equilibria involving calcium carbonate at high pressure. American Journal of Science, 260, 374–382.

Caciagli, N.C. (2001) The solubility of calcite in water at 5–16 kilobars and 500–800 °C. M.Sc. Thesis, University of California, Los Angeles.

Carmichael, I.S.E. (1991) The redox states of basic and silicic magmas: a reflection of their source regions? Contributions to Mineralogy and Petrology, 106, 129–144.

Chadwick, B., Ramakrishnan, M., Vasudev, V.N., and Viswanatha, M.N. (1989) Facies distributions and structure of a Dharwar volcanosedimentary basin: evidence for Late Archean transpression in southern India. Journal of the Geological Society of London, 146, 825–834.

Clark, S.P., Jr. (1959) Effect of pressure on the melting point of eight alkali halides. Journal of Chemical Physics, 31, 1526–1531.

Craw, D., Rattenbury, M.S., and Johnstone, R.D. (1987) Structural geology and vein mineralization in the Callery River headwaters, Southern Alps, New Zealand. New Zealand Journal of Geology and Geophysics, 30, 273–286.

Crawford, M.L. and Hollister, L.S. (1986) Metamorphic fluids, the evidence from fluid inclusions. In J.V. Walther and B.J. Wood, Eds., Fluid-Rock Interactions During Metamorphism, 1–35. Springer, New York.

Dahlgren, S., Bogoch, R., Magaritz, M., and Michard, A. (1993) Hydrothermal dolomite marbles associated with charnockitic magmatism in the Proterozoic Bamble Shear Belt, south Norway. Contributions to Mineralogy and Petrology, 113, 394–408.

De Jong, G. and Williams, P.C. (1995) Giant metasomatic system formed during exhumation of midcrustal Proterozoic rocks in the vicinity of the Cloncurry fault, northwest Queensland. Australian Journal of Earth Sciences, 42, 281–290.

Edwards, A.B. and Baker, G. (1953) Scapolitization in the Cloncurry District of north-western Queensland. Journal of the Geological Society of Australia, 1, 1–33.

Ellis, A.J. (1959) The solubility of calcite in carbon dioxide solutions. American Journal of Science, 257, 354–365.

———(1963) The solubility of calcite in sodium chloride solutions at high temperatures. American Journal of Science, 261, 259–267.

Ellis, D.E. (1978) Stability and phase equilibria of chloride and carbonate bearing scapolites at 750 °C and 4000 bar. Geochimica et Cosmochimica Acta, 42, 1271–1281.

Fein, J.B. and Walther, J.V. (1987) Calcite solubility in supercritical CO_2-H_2O fluids. Geochimica et Cosmochimica Acta, 51, 1665–1673.

———(1989) Calcite solubility and speciation in supercritical NaCl-HCl aqueous fluids. Contributions to Mineralogy and Petrology, 103, 317–324.

Franz, L. and Harlov, D.E. (1998) High-grade K-feldspar veining in granulites from the Ivrea-Verbano Zone, northern Italy: fluid flow in the lower crust and implications for granulite facies genesis. Journal of Geology, 106, 455–472.

Gittins, J., Beckett, M.F., and Jago, B.C. (1990) Composition of the fluid phase accompanying carbonatite magma: a critical examination. American Mineralogist, 75, 1106–1109.

Hansteen, T.H. and Burke, E.A.J. (1990) Melt-mineral-fluid interaction in the Oslo Rift, southeast Norway: II. High-temperature fluid inclusions in the Eikern-Skrim complex. Norges Geologiske Undersökelse Bulletin, 417, 15–32.

Harlov, D.E., Newton, R.C., Hansen, E.C., and Janardhan, A.S. (1997) Oxide and sulphide minerals in highly oxidized, Rb-depleted Archean granulites of the Shevaroy Hills Massif, south India: Oxidation states and the role of metamorphic fluids. Journal of Metamorphic Geology, 15, 701–717.

Henry, C., Burkhard, M., and Goffe, B. (1996) Evolution of synmetamorphic veins and their wallrocks through a western Alps transect; no evidence for large-scale fluid flow; stable isotope, major- and trace-element systematics. Chemical Geology, 127, 81–109.

Herms, P. and Schenk, V. (1998) Fluid inclusions in high-pressure granulites of the Pan-African belt in Tanzania (Uluguru Mts.): a record of prograde to retrograde fluid evolution. Contributions to Mineralogy and Petrology, 130, 199–212.

Izraeli, E.S., Harris, J.W., and Navon, O. (2001) Brine inclusions in diamonds: a new upper mantle fluid. Earth and Planetary Science Letters, 187, 323–332.

Koster Van Groos, A.F. (1991) Differential thermal analysis of the liquidus relations in the system NaCl-H_2O to 6 kbar. Geochimica et Cosmochimica Acta, 55, 2811–2817.

Lapin, A.V. and Ploshko, V.V. (1988) Rock-association and morphological types of carbonatites and their geotectonic environments. International Geology Review, 30, 390–396.

Lapin, A.V., Ploshko, V.V., and Malyshev, A.A. (1987) Carbonatites of the Tatar deep-seated fault zone, Siberia. International Geology Review, 29, 551–567.

Markl, G. and Bucher, K. (1998) Composition of fluids in the lower crust inferred from metamorphic salt in lower crustal rocks. Nature, 391, 781–783.

Morogan, V. and Woolley, A.R. (1988) Fenitization in the Alnö complex, Sweden: distribution, mineralogy and genesis. Contributions to Mineralogy and Petrology, 100, 169–182.

Newton, R.C. and Manning, C.E. (2000) Quartz solubility in H_2O-NaCl and H_2O-CO_2 solutions at deep crust-upper mantle pressures and temperatures: 2–15 kbar and 500–900 °C. Geochimica et Cosmochimica Acta, 64, 2993–3005.

Newton, R.C., Aranovich, L.Y., Hansen, E.C., and Vandenheuvel, B.A. (1998) Hypersaline fluids in Precambrian deep-crustal metamorphism. Precambrian Research, 91, 41–63.

Niggli, P. (1919) Untersuchungen an Karbonat- und Chloridschmelzen. Zeitschrift für Anorganische und Allegemeine Chemie, 106, 126–142.

Nozhkin, A.D. and Turkina, O.M. (1995) Radiochemistry of the charnockite-granulite complex, Sharyzhalgay Window, Siberian Platform. Geochemistry International, 32, 62–78.

Oliver, N.H.S., Cartwright, I., Wall, V.J., and Golding, S.D. (1993) The stable isotope signature of kilometer-scale fracture-dominated metamorphic fluid pathways, Mary Kathleen, Australia. Journal of Metamorphic Geology, 11, 705–720.

Philippot, P. and Selverstone, J. (1991) Trace-element-rich brines in eclogitic veins: implications for fluid composition and transport during subduction. Contributions to Mineralogy and Petrology, 106, 417–430.

Scambelluri, M., Pennachioni, G., and Philippot, P. (1998) Salt-rich aqueous fluids formed during eclogitization of metabasalts in the Alpine continental crust (Austroalpine Mt. Emilius unit, Italian western Alps). Lithos, 43, 151–167.

Shmulovich, K.I. and Graham, C.M. (1996) Melting of albite and dehydration of brucite in H_2O-NaCl fluids to 9 kbars and 700–900 °C: implications for partial melting and water activities during high pressure metamorphism. Contributions to Mineralogy and Petrology, 124, 370–382.

Stern, R.J. and Gwinn, C.J. (1990) Origin of Late Precambrian intrusive carbonates, eastern desert of Egypt and Sudan: C, O and Sr isotope evidence. Precambrian Research, 46, 259–272.

Touret, J.L.R. (1985) Fluid regime in southern Norway: the record of fluid inclusions. In A.C. Tobi and J.L.R. Touret, Eds., The Deep Proterozoic Crust in the North Atlantic Provinces, 517–549. Reidel, Dordecht, The Netherlands.

Wickham, S.M., Janardhan, A.S., and Stern, R.J. (1994) Regional carbonate alteration of the crust by mantle-derived magmatic fluids, Tamil Nadu, South India. Journal of Geology, 102, 379–398.

Wyllie, P.J. and Tuttle, O.F. (1960) The system CaO-CO_2-H_2O and the origin of carbonatites. Journal of Petrology, 1, 1–46.

MANUSCRIPT RECEIVED SEPTEMBER 18, 2001
MANUSCRIPT ACCEPTED JUNE 10, 2002
MANUSCRIPT HANDLED BY GRAY E. BEBOUT